Journal of Power Sources 211 (2012) 84–91

Contents lists available at SciVerse ScienceDirect

Journal of Power Sources

journal homepage: www.elsevier.com/locate/jpowsour

Electrochemical properties of spherically shaped dense V_2O_5 cathode powders prepared directly by spray pyrolysis

You Na Ko, Jung Hyun Kim, Seung Ho Choi, Yun Chan Kang*

Department of Chemical Engineering, Konkuk University, 1 Hwayang-dong, Gwangjin-gu, Seoul 143-701, Republic of Korea

ARTICLE INFO

Article history:
Received 21 January 2012
Received in revised form
13 March 2012
Accepted 16 March 2012
Available online 10 April 2012

Keywords:
Cathode material
Spray pyrolysis
Vanadium pentoxide
Lithium battery

ABSTRACT

Spherically shaped vanadium pentoxide (V_2O_5) cathode powders with porous or dense morphologies are prepared directly via spray pyrolysis by varying the preparation temperatures between 600 and 1000 °C. The powders prepared at 600 °C consist of nanometer-sized rod-shaped crystals with porous structures. The V_2O_5 powders prepared at 1000 °C have spherical shapes, clean surfaces, and dense structures, because of complete melting of the powders that occurs inside the hot-wall reactor. The Brunauer–Emmett–Teller (BET) surface areas of the V_2O_5 powders decrease from 24.7 to 3.2 $m^2 g^{-1}$ when the preparation temperature increases from 600 to 1000 °C. The V_2O_5 powders prepared at 1000 °C have better cycle properties than those prepared at 600 and 800 °C. The discharge capacity of the V_2O_5 powders prepared at 1000 °C decreases from 432 mAh g^{-1} to 263 mAh g^{-1} after 20 cycles, in which the capacity retention is 61%.

1. Introduction

The increasing demand for high power density, high energy efficiency, and good rate performance from lithium ion batteries has prompted extensive investigation of alternative cathode materials [1]. Vanadium pentoxide (V_2O_5) is considered to be a good cathode candidate for lithium ion batteries because of its low cost and high theoretical capacity that reaches 440 mAh g^{-1} when three lithium ions are intercalated per mole of V_2O_5 [2–5].

However, the practical application of V_2O_5 as a cathode is restricted by the dissolution of vanadium into the electrolyte, which leads to rapid capacity fading on cycling [6–10]. To prevent the dissolution of vanadium, various studies were performed [11–16]. Chou et al. investigated the electrochemical performances of the porous V_2O_5 nanoribbon cathode material combined with a room temperature ionic liquid (RTIL) electrolyte [11]. The results show that the RTIL can prevent the dissolution of V_2O_5 during charge and discharge processes. Dawei et al. prepared the Al_2O_3-deposited V_2O_5 xerosol films [12]. During the cycles, atomic layer of Al_2O_3 which were coated onto V_2O_5 surface could prevent V_2O_5 electrode dissolution into electrolyte by reducing direct contact between active electrode and electrolyte. And conducting polymers are studied as coating material for electrode materials to improve the electronic conductivity and prevent the electrode dissolution in acidic medium [13–16]. Zhao et al. synthesized composites of V_2O_5 and polypyrrole (PPy) by hydrothermal reduction [13]. PPy modification of the V_2O_5 cathode improved cyclic performance.

Reducing the specific surface area of the cathode powder is efficient in decreasing the dissolution of vanadium, due to reduction in the active material-electrolyte interface area. To synthesize V_2O_5 cathode powders with low surface areas, high preparation temperatures are required.

Generally, V_2O_5 cathode powders have been prepared by liquid solution methods [17–21]. However, liquid solution methods requiring a post-treatment process have the disadvantage of low preparation temperatures, which are not suitable for the preparation of cathode powders with low surface areas. High post-treatment temperatures result in the formation of V_2O_5 cathode powders with large sizes and irregular morphologies, because of the low melting temperature (690 °C) of V_2O_5.

Spray pyrolysis is suitable for the preparation of cathode powders with fine-sized, non-aggregated, spherical, and dense morphologies [22–26]. Feng et al. prepared V_2O_5 cathode powders by spray pyrolysis at a low temperature (350 °C) [26]. The V_2O_5 powders post-treated at 420 °C had spherical shapes and high surface area (114 $m^2 g^{-1}$). However, during spray pyrolysis, the morphologies and specific surface areas of the V_2O_5 powders could be controlled by changing preparation conditions, such as preparation temperatures and the flow rates of the carrier gas. In this study, V_2O_5 cathode materials with differing morphologies and surface areas were prepared directly by spray pyrolysis under various preparation conditions. In particular, the effects of the

* Corresponding author. Tel.: +82 2 2049 6010; fax: +82 2 458 3504.
E-mail address: yckang@konkuk.ac.kr (Y.C. Kang).

0378-7753/$ – see front matter © 2012 Elsevier B.V. All rights reserved.
doi:10.1016/j.jpowsour.2012.03.072

preparation temperature on the morphologies, surface areas, and electrochemical properties of the V_2O_5 powders were investigated. The V_2O_5 cathode powders prepared at a high temperature (above the melting temperature of V_2O_5) had spherical shapes, high crystallinity, low surface areas, and good electrochemical properties.

2. Experimental

The precursor solution was prepared by dissolving vanadium pentoxide in distilled water and nitric acid with heating, to obtain a V_2O_5 concentration of 0.08 M. The V_2O_5 powders were prepared directly by ultrasonic spray pyrolysis at 600, 800, and 1000 °C without post-treatment. The schematic diagram of the equipment is shown in Fig. 1. The spray pyrolysis system consists of a droplet generator, a quartz reactor, and a teflon bag filter (powder collector). A 1.7 MHz ultrasonic spray generator having six vibrators was used to generate a large amount of droplets, which are carried into the high temperature tubular reactor by a carrier gas. The length and diameter of the quartz reactor are 1200 and 50 mm, respectively. The length of a single zone heating furnace was 60 cm. The flow rate of air used as the carrier gas was varied between 10 and 60 L min^{-1}.

The morphological characteristics of the powders were investigated by scanning electron microscopy (SEM, JEOL JSM-6060) and field emission scanning electron microscopy (FE-SEM, HITACHI, S-4300). The crystal structures of the V_2O_5 powders were investigated by X-ray diffractometry (XRD, X'Pert PRO MPD) using Cu Kα radiation ($\lambda = 1.5418$ Å). The specific surface areas of the V_2O_5 powders were measured according to the Brunauer–Emmett–Teller (BET) method and the pore size distributions were calculated using the Barrett–Joyner–Halenda (BJH) model. The capacities and cycle properties of the V_2O_5 cathode powders were measured using a 2032-type coin cell. The cathode electrode was prepared from a mixture of 20 mg V_2O_5 and 12 mg TAB (TAB is a mixture of 9.6 mg teflonized acetylene black and 2.4 mg binder). Lithium metal and a microporous polypropylene film were used as the anode and the separator, respectively. The electrolyte was 1 M $LiPF_6$ in a 1:1 mixture by volume of ethylene carbonate (EC)/dimethyl carbonate (DMC). The charge/discharge characteristics of the samples were investigated during cycling in the 1.5–4 V potential range at constant current densities of 29.4 and 294 mA g^{-1}.

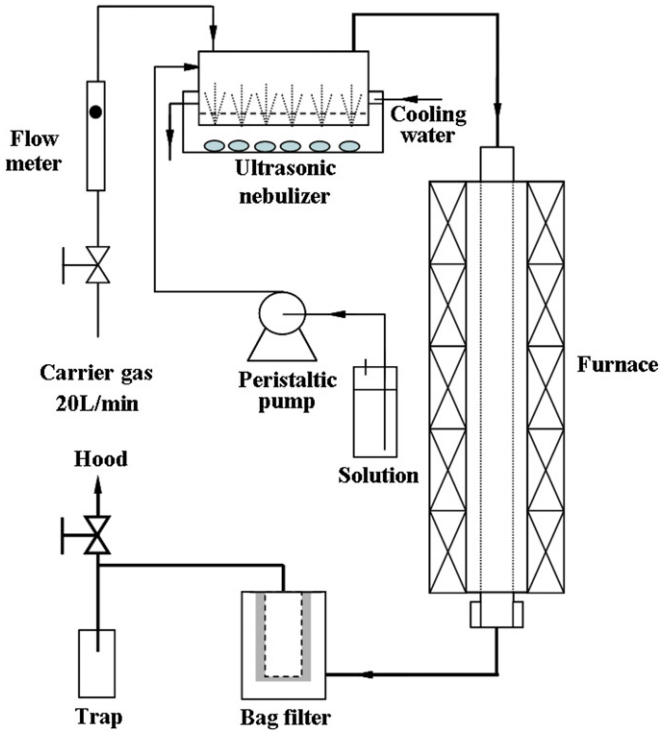

Fig. 1. Schematic diagram of the spray pyrolysis process.

3. Results and discussion

The characteristics of the powders prepared by spray pyrolysis were affected by the preparation temperature and powder residence time inside the hot-wall reactor. In particular, the morphologies and specific surface areas of the V_2O_5 powders were sensitively affected by the preparation conditions because of the low crystallization and melting temperatures of V_2O_5. The melting temperature of V_2O_5 is low as 690 °C. The morphologies of the V_2O_5 powders prepared at various temperatures were investigated by SEM, FE-SEM, and TEM (Figs. 2–4). The V_2O_5 powders obtained by spray pyrolysis at a constant carrier-gas flow rate of 20 L min^{-1} had spherical morphologies irrespective of the preparation temperature. During spray pyrolysis, one powder particle was formed from one droplet by the drying, decomposition, and crystallization or melting processes inside the hot-wall reactor. Thus, the spherically shaped V_2O_5 powders prepared at a low temperature (600 °C) were composed of nanometer-sized rod-shaped crystals because of the low crystallization temperature of V_2O_5. The V_2O_5 powders prepared at 800 °C were also composed of rod-shaped crystals, but the crystals had grown more than the powders prepared at 600 °C and the crystals were partially melted (Fig. 3b). The V_2O_5 powders prepared at 1000 °C displayed a bimodal size distribution of nanosized and micron-sized powders (Fig. 3c).

The morphologies of the V_2O_5 powders prepared at 1000 °C with different carrier-gas flow rates were investigated to probe their formation mechanisms. Fig. 5 shows the SEM images of the V_2O_5 powders prepared by spray pyrolysis at 1000 °C and at carrier-gas flow rates of 10, 40, and 60 L min^{-1}. The residence time of the powder inside the hot-wall reactor decreased from 1.7 to 0.3 s when the carrier-gas flow rate was varied from 10 to 60 L min^{-1}. The V_2O_5 powders prepared at the high carrier-gas flow rate of 60 L min^{-1} had spherical morphology and a smooth surface due to the formation of fine rod-shaped crystals. Growth of the rod-shaped V_2O_5 crystals did not occur at 1000 °C because of the short residence time of the powder inside the hot-wall reactor. When the carrier-gas flow rate was 40 L min^{-1}, growth of the rod-shaped crystals resulted in V_2O_5 powders with porous structures and rough surfaces, as indicated by arrows in Fig. 5b. The V_2O_5 powders prepared at the low carrier-gas flow rate of 10 L min^{-1} had spherical shapes, clean surfaces, and dense structures, because of complete melting of the powders that occurred inside the hot-wall reactor. Some of the rod-shaped particles converted into nanosized particles on the surface of the submicron-sized V_2O_5 powders. The formation mechanism of the V_2O_5 powders during the spray pyrolysis according to the preparation temperature is described in Fig. 6.

The crystal structures of V_2O_5 powders directly prepared by spray pyrolysis at various temperatures are shown in Fig. 7. The flow rate of the carrier gas was 20 L min^{-1}. Irrespective of the preparation temperature, the XRD pattern of each powder corresponds to the orthorhombic structure of V_2O_5 (JCPDS 41-1426). No impurity peaks were detected. However, the powders prepared at 600 °C had poor crystallinity because of short residence time of the powders inside the hot-wall reactor. The mean

crystallite sizes of the powders prepared at 600, 800, and 1000 °C, calculated from the (001) peak widths using Scherrer's equation, were 19, 31, and 28 nm, respectively. Complete melting of the powders slightly decreased their mean crystallite size. Fig. 8 shows the thermogravimetry (TG) and differential scanning calorimetry (DSC) curves of the V_2O_5 powders obtained at 600, 800, and 1000 °C. The TG curves of these powders prepared at 600 and 800 °C showed that they had slight weight losses because of the loss of adsorbed water molecules. However, no exothermic or endothermic peaks were observed in the DSC curves of these samples. From the TG and DSC results, it was confirmed that the precursor component was completely decomposed despite the short residence time of the powders inside the reactor maintained at 600 °C.

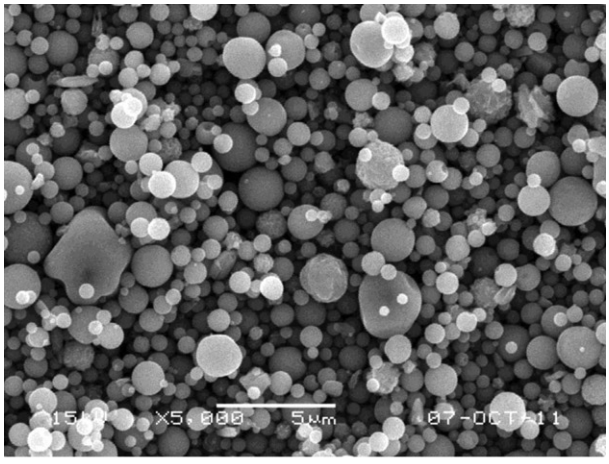

a 600°C

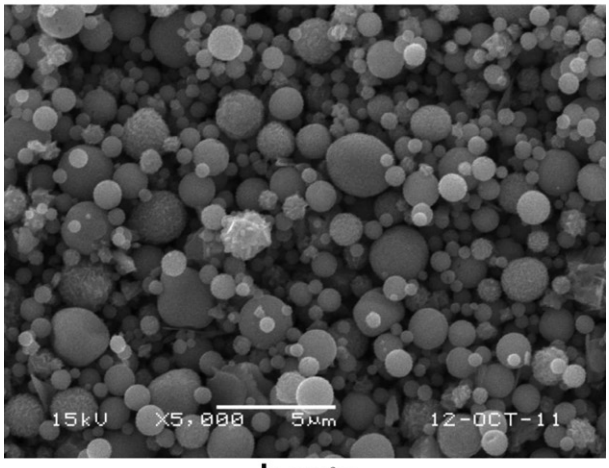

b 800°C

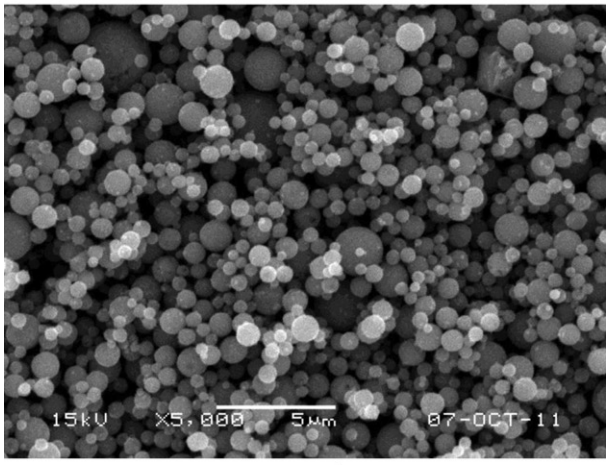

c 1000°C

Fig. 2. SEM images of the V_2O_5 powders prepared by spray pyrolysis at various temperatures.

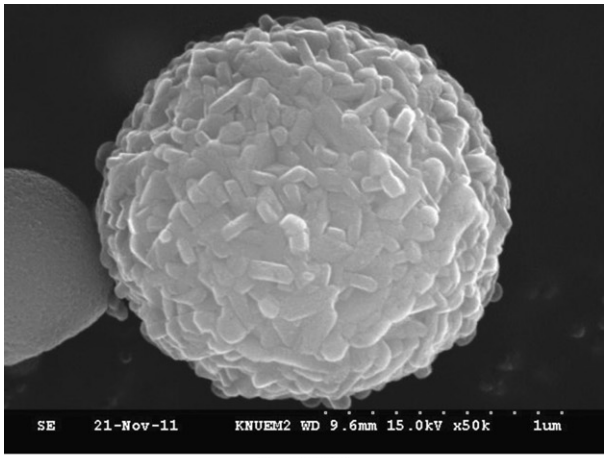

a 600°C

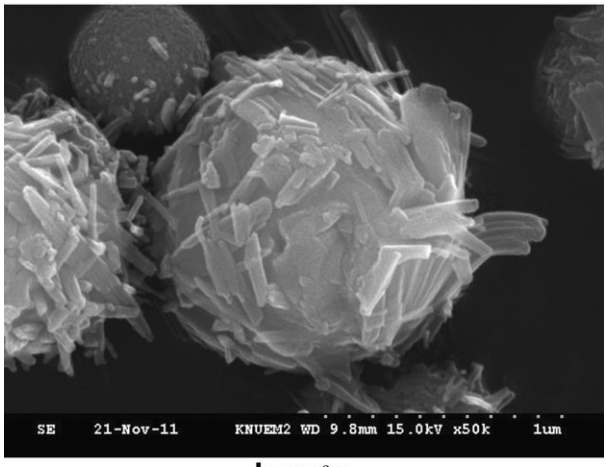

b 800°C

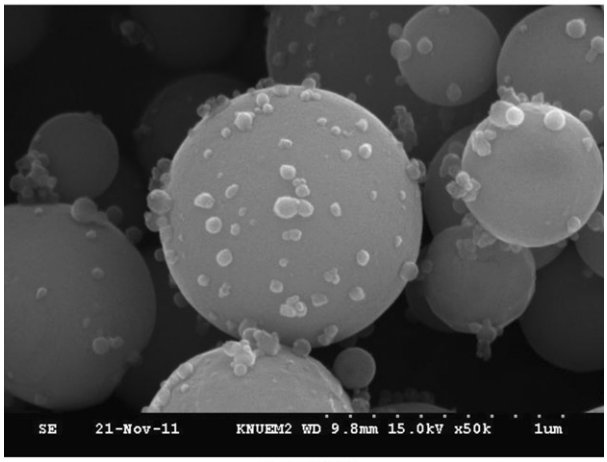

c 1000°C

Fig. 3. FE-SEM images of the V_2O_5 powders prepared by spray pyrolysis at various temperatures.

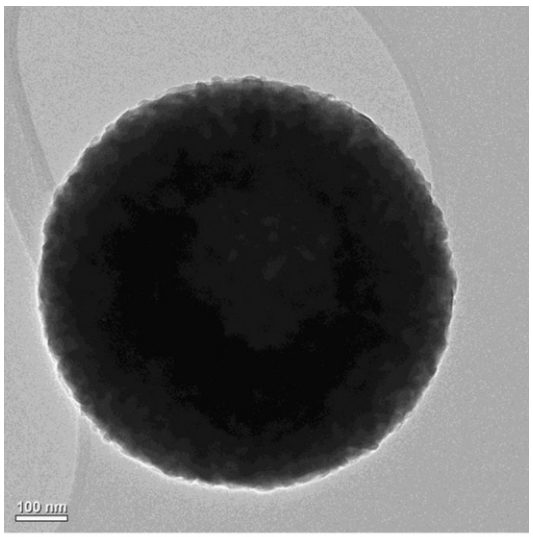

a 600°C

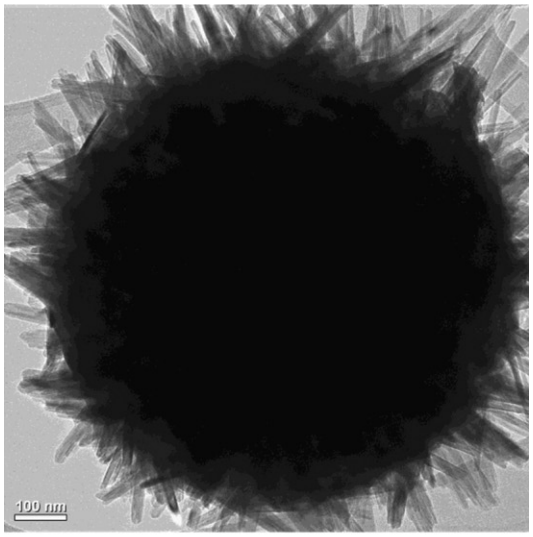

b 800°C

c 1000°C

Fig. 4. TEM images of the V_2O_5 powders prepared by spray pyrolysis at various temperatures.

The pore structures of the spherical V_2O_5 powders also were affected by the preparation temperature when the flow rate of the carrier gas was 20 L min^{-1}. The BJH pore size distributions of the V_2O_5 powders obtained at different temperatures were investigated, as shown in Fig. 9. The V_2O_5 powders prepared at 600 and 800 °C contained mesopores with pore sizes between 3 and 5 nm.

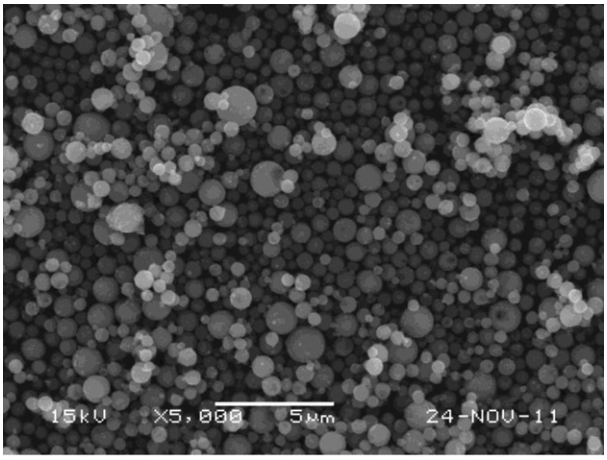

a 10 L•min^{-1}

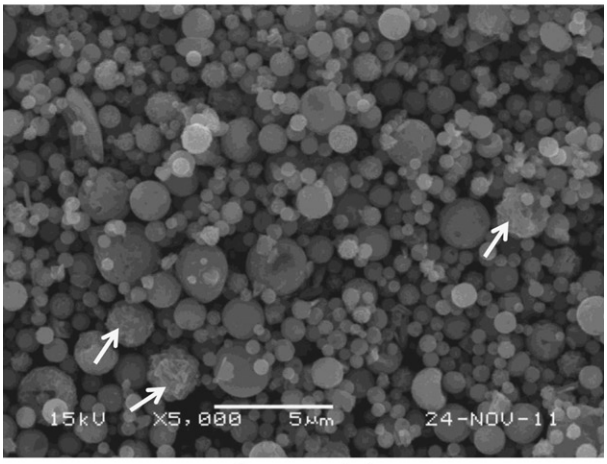

b 40•L min^{-1}

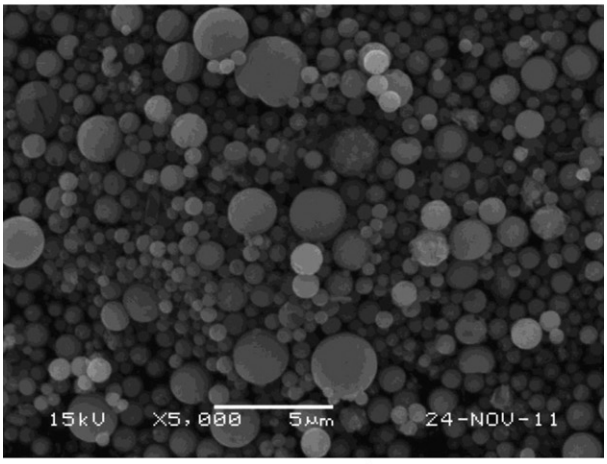

c 60 L•min^{-1}

Fig. 5. SEM images of the powders prepared by spray pyrolysis at various carrier-gas flow rates at 1000 °C.

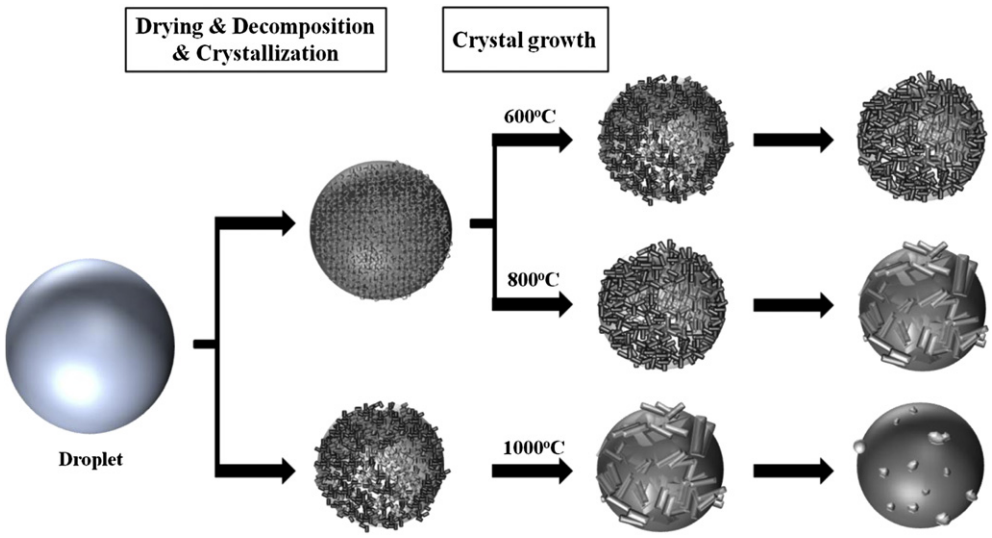

Fig. 6. Schematic diagram of the formation of the V_2O_5 powders in the spray pyrolysis.

The pore volumes of the powders prepared at 600 and 800 °C were 0.039 and 0.044 $cm^3\ g^{-1}$, respectively. However, the V_2O_5 powders prepared at 1000 °C had dense structures without pores. The BET surface areas of the V_2O_5 powders prepared at 600, 800, and 1000 °C were 24.7, 13.5, and 3.2 $m^2\ g^{-1}$, respectively.

The electrochemical performances of the V_2O_5 powders prepared by spray pyrolysis at various temperatures were investigated in the voltage range of 1.5–4 V at a constant current density of 29.4 mA g^{-1}. The flow rate of the carrier gas was 20 L min^{-1}. Initial charge/discharge curves are shown in Fig. 10. The V_2O_5 powders prepared at 600, 800, and 1000 °C had high initial discharge capacities of 404, 427, and 432 mAh g^{-1}, respectively. The initial charge capacities were 355, 385, and 375 mAh g^{-1} when the preparation temperatures of the powders were 600, 800, and 1000 °C, respectively. The poor crystallinity and adsorbed water molecules decreased the first charge and discharge capacities of the powders prepared at a low temperature of 600 °C. Irrespective of the preparation temperatures, four plateaus were observed in the initial discharge curves that relate to phase transitions between α-$Li_xV_2O_5$ ($x < 0.01$), ε-$Li_xV_2O_5$ ($0.35 < x < 0.7$), δ-$Li_xV_2O_5$ ($x = 1$), γ-$Li_xV_2O_5$ ($1 < x < 2$), and ω-$Li_xV_2O_5$ ($2 < x \leq 3$) [20,27]. The V_2O_5 powders prepared at 1000 °C had larger initial charge and discharge capacities than those prepared at 600 and 800 °C. Subsequent charge/discharge performances and incremental capacity curves of the V_2O_5 powders prepared at 1000 °C are shown in Fig. 11. The distinct reduction peaks at 3.32, 3.11, 2.26, and 1.93 V in the first incremental capacity curve are indicative of the formation of ε-$Li_xV_2O_5$, δ-$Li_xV_2O_5$, γ-$Li_xV_2O_5$, and ω-$Li_xV_2O_5$ phases, respectively. After the irreversible ω-$Li_xV_2O_5$ phase is formed at a low voltage in the initial lithiation process, Li^+ cannot be completely removed during the initial delithiation process [27,28]. Thus, the V_2O_5 cathode powder had a low discharge capacity (325 mA h g^{-1}) at the second cycle, and the plateaus shown in the initial discharge curve disappeared in the subsequent discharging curves. During subsequent cycles, there were only single broad reduction/oxidation peaks at around 2.35/2.58 V, as shown in Fig. 11b. These peaks indicated the reversibility of the oxidation/reduction reactions. Fig. 12 shows the XRD patterns of the V_2O_5 cathode before and after electrochemical test. The crystal structures of the cathode samples which formed from the V_2O_5 powders prepared at 1000 °C and teflonized acetylene black before and after

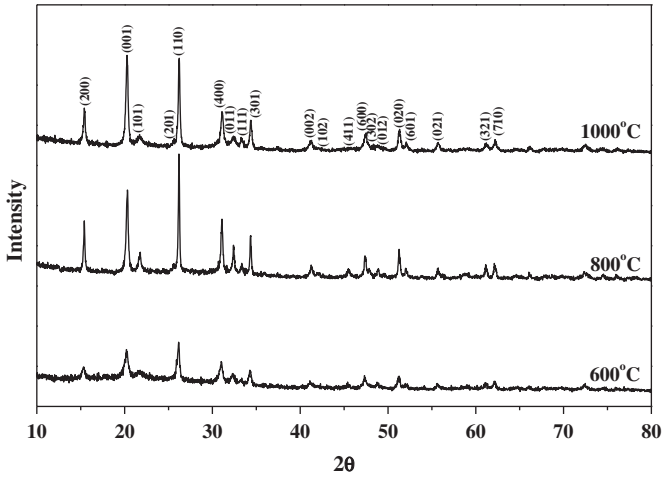

Fig. 7. XRD patterns of the V_2O_5 powders prepared by spray pyrolysis at various temperatures.

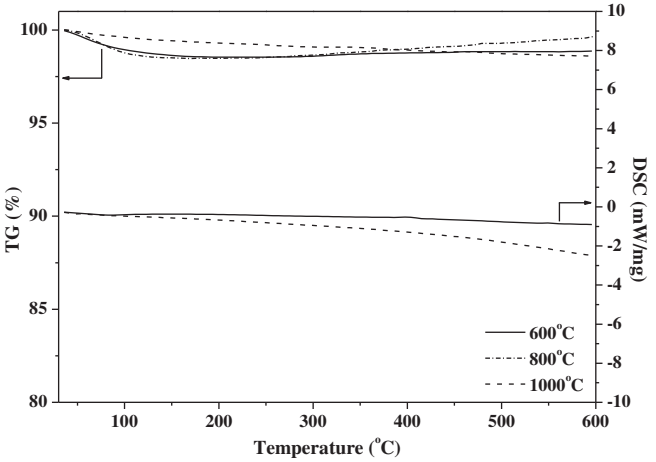

Fig. 8. TG/DSC curves of the V_2O_5 powders prepared by spray pyrolysis at various temperatures.

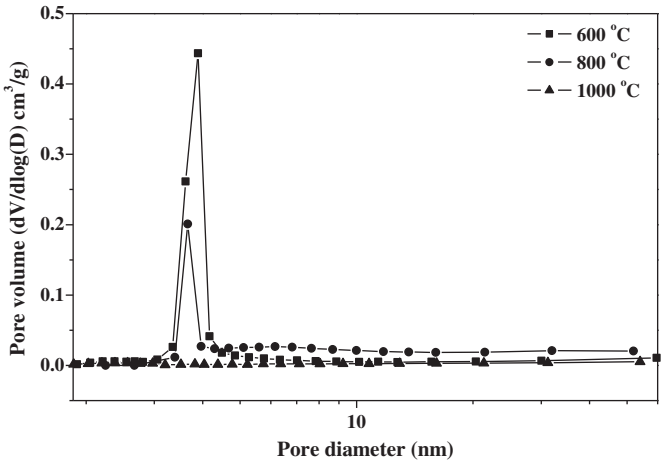

Fig. 9. Pore size distributions of the V_2O_5 powders prepared by spray pyrolysis at various temperatures.

electrochemical test were investigated at fully charged or discharged state. The crystal structure of the cathode samples changed after first cycle. However, the cathode samples had the same crystal structure after electrochemical test irrespective of the cycle numbers. Therefore, the charge and discharge curves of the cathode had the same shape irrespective of the cycle numbers from the second charge/discharge cycle.

Cycle properties of the V_2O_5 powders prepared at various temperatures are shown in Fig. 13. Regardless of the preparation temperatures, the V_2O_5 powders prepared by spray pyrolysis had large first irreversible capacity losses which resulted from the formation of the irreversible phase. After 20 cycles, the discharge capacities of the V_2O_5 cathode powders prepared at 600, 800, and 1000 °C decreased to 229, 212, and 263 mAh g^{-1}, respectively. The capacity retentions of the powders prepared at 600, 800, and 1000 °C were 57, 50, and 61%, respectively. The V_2O_5 powders prepared at 1000 °C had better cycle properties as a result of low pore volume and low specific surface area, which reduced the active material–electrolyte interface area and the dissolution of vanadium.

First and second charge/discharge performances of the V_2O_5 powders at a constant current density of 294 mA g^{-1} are shown in

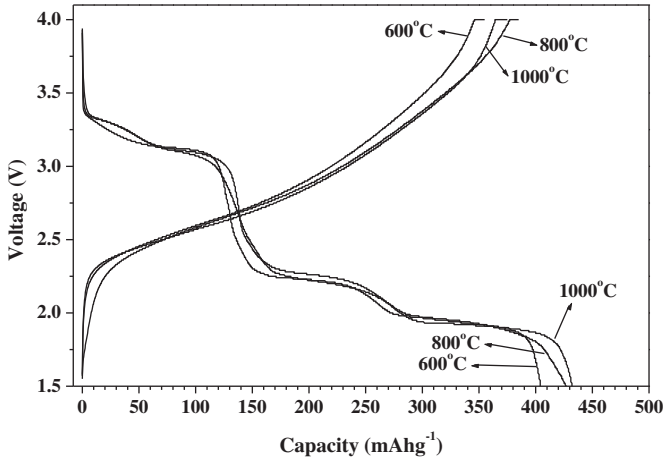

Fig. 10. Initial charge/discharge curves of the V_2O_5 powders prepared at various temperatures at a constant current density of 29.4 mA g^{-1}.

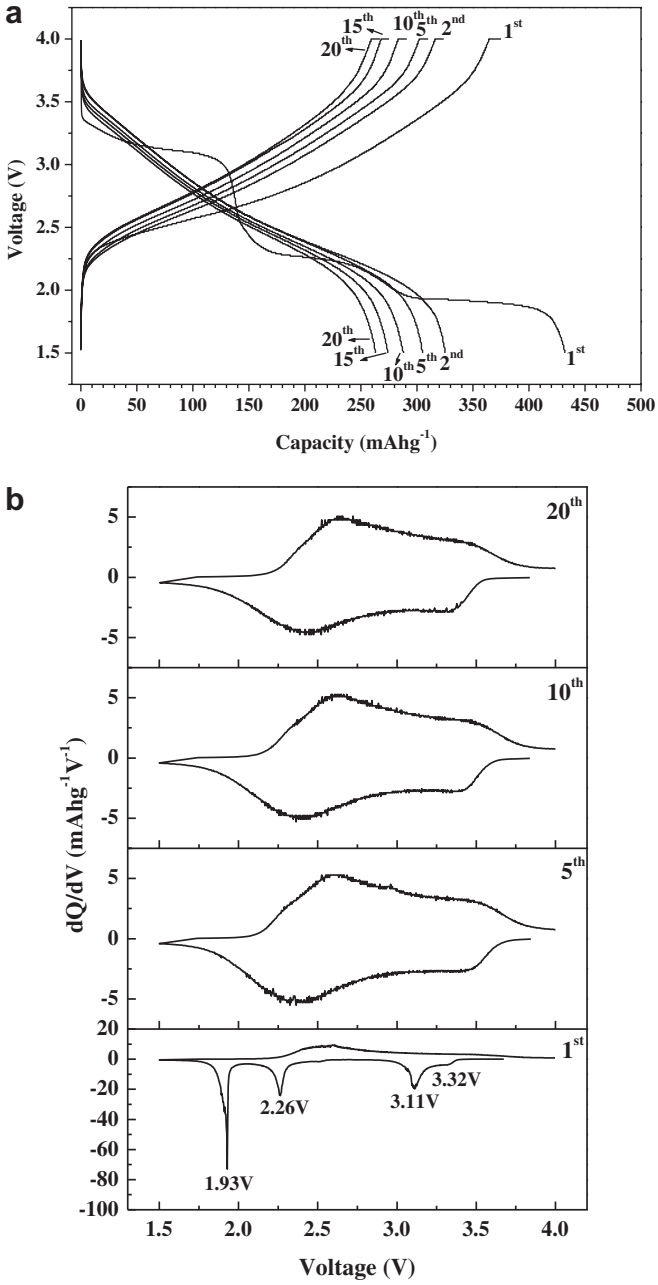

Fig. 11. Subsequent charge/discharge curves (a) and incremental capacity curves (dQ/dV) (b) of the V_2O_5 powders prepared at 1000 °C.

Fig. 14. The V_2O_5 powders prepared at 600, 800, and 1000 °C had initial discharge capacities of 281, 247, and 174 mAh g^{-1}, respectively. In contrast to the initial discharge capacities of the powders at a constant current density of 29.4 mA g^{-1}, V_2O_5 powders prepared at 600 °C had higher capacity than those of V_2O_5 powders prepared at 800 and 1000 °C. This is due to the improvement of the electrochemical performance of the V_2O_5 powders prepared at 600 °C as a result of high surface area and short Li-diffusion path. The poor electronic conductivity (10^{-2} to 10^{-3} S cm^{-1}) and low diffusion coefficient of lithium ions ($D \sim 10^{-12}$ cm^2 s^{-1}) in vanadium oxide are known to lead to poor electrochemical performance at high current densities [29–31]. The Coulombic efficiency was calculated by dividing the charge capacity by discharge capacity. The Coulombic efficiencies of the

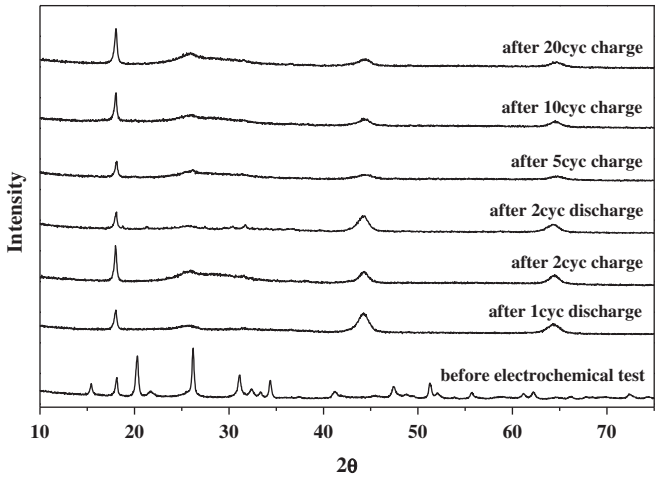

Fig. 12. XRD patterns of the cathode samples before and after electrochemical test.

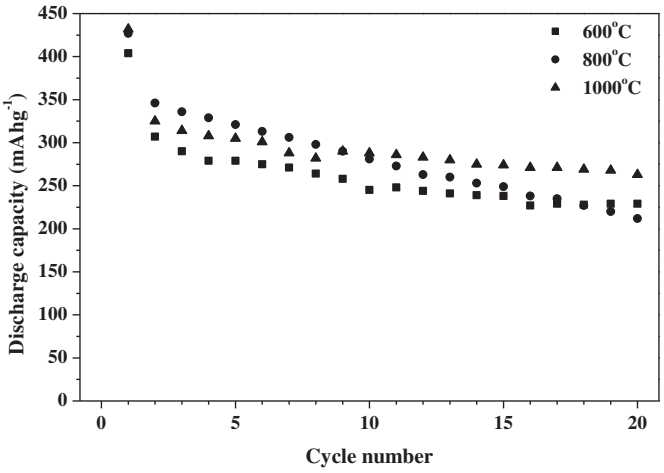

Fig. 13. Cycle properties of the V_2O_5 powders prepared by spray pyrolysis at various temperatures at a constant current density of 29.4 mA g^{-1}.

V_2O_5 cathode powders prepared at 600, 800, and 1000 °C were 80, 89, and 83%, in the first cycle. The cathode powders prepared at 600 °C had a low Coulombic efficiency because of low crystallinity and high surface area by increasing the dissolution characteristics of V component. The high current rate decreased the Coulombic efficiency of the V_2O_5 cathode powders with dense structure without pores.

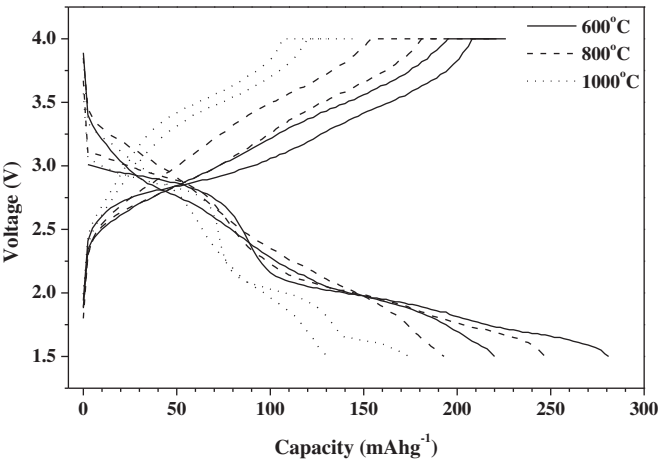

Fig. 14. First and second charge/discharge curves of the V_2O_5 powders prepared at various temperatures at a constant current density of 294 mA g^{-1}.

4. Conclusions

The physical and electrochemical properties of V_2O_5 powders prepared directly by spray pyrolysis were investigated. The powders had a pure phase corresponding to the V_2O_5 crystal irrespective of the preparation temperature. However, the morphologies and electrochemical properties were affected by the preparation temperatures of the powders. The V_2O_5 powders prepared at 600 °C had porous nanostructures and high BET surface areas. In comparison, the V_2O_5 powders prepared at 1000 °C had dense structures without pores and small BET surface areas. The V_2O_5 powders with dense structures, high crystallinity and low adsorbed water molecules had large initial discharge capacities and good cycle properties at a low current density, as a result of the reduction of the active material-electrolyte interface area and the dissolution of vanadium. However, the V_2O_5 powders prepared at 600 °C with high surface area had higher discharge capacity than those of V_2O_5 powders prepared at 800 and 1000 °C.

Acknowledgment

This research was supported by the Converging Research Center Program through the National Research Foundation of Korea (NRF) funded by the Ministry of Education, Science and Technology (2011-50210). This study was also supported by a grant (M2009010025) from the Fundamental R&D Program for Core Technology of Materials funded by the Ministry of Knowledge Economy (MKE), Republic of Korea. This study was also supported by Seoul R&BD Program (WR090671).

References

[1] J.W. Fergus, J. Power Sources 195 (2010) 939.
[2] E.A. Ponzio, T.M. Benedetti, R.M. Torresi, Electrochim. Acta 52 (2007) 4419.
[3] N.A. Chernova, M. Roppolo, A.C. Dillon, M.S. Whittingham, J. Mater. Chem. 19 (2009) 2526.
[4] Y. Wang, K. Takahashi, K. Lee, G.Z. Cao, Adv. Funct. Mater. 16 (2006) 1133.
[5] T. Zhai, H. Liu, H. Li, X. Fang, N. Liao, L. Li, H. Zhou, Y. Koide, Y. Bando, D. Golberg, Adv. Mater. 22 (2010) 2547.
[6] G. Sudant, E. Baudrin, B. Dunn, J.M. Tarascon, J. Electrochem. Soc. 151 (2004) A666.
[7] E. Baudrin, G. Sudant, D. Larcher, B. Dunn, J.M. Tarascon, Chem. Mater. 18 (2006) 4369.
[8] Y.S. Cohem, D. Aurbach, Electrochem. Commun. 6 (2004) 536.
[9] D. Aurbach, B. Markovsky, G. Salitra, E. Markevich, Y. Talyossef, M. Koltypin, L. Nazar, B. Ellis, D. Kovacheva, J. Power Sources 165 (2007) 491.
[10] S. Patoux, C. Wurm, M. Morcrette, G. Rousse, C. Masquelier, J. Power Sources 119–121 (2003) 278.
[11] S.L. Chou, J.Z. Wang, J.Z. Sun, D. Wexler, M. Forsyth, H.K. Liu, D.R. MacFarlane, S.X. Dou, Chem. Mater. 20 (2008) 7044.
[12] D. Liu, Y. Liu, S.L. Stephanie, G. Cao, J. Liu, Y.H. Jeong, J. Vac. Sci. Technol 30 (2012) 01A123.
[13] H. Zhao, A. Yuan, B. Liu, S. Xing, X. Wu, J. Xu, J. Appl. Electrochem 42 (2012) 139.
[14] F. Huguenin, R.M. Torresi, J. Phys. Chem. C 112 (2008) 2202.
[15] H.M. Song, Y. Kim, Q.T. Ta, I.H. Yeo, W.I. Cho, S.I. Mho, ECS Trans. 28 (2010) 117.
[16] H.P. Wong, B.C. Dave, F. Leroux, J. Harreld, B. Dunn, L.F. Nazar, J. Mater.Chem. 8 (1998) 1019.
[17] S. Wang, Z. Lu, D. Wang, C. Li, C. Chen, Y. Yin, J. Mater. Chem. 21 (2011) 6365.
[18] A.M. Cao, J.S. Hu, H.P. Liang, L.J. Wan, Angew. Chem. 117 (2005) 4465.
[19] Y.L. Cheah, N. Gupta, S.S. Pramana, V. Aravindan, G. Wee, M. Srinivasan, J. Power Sources 196 (2011) 6465.
[20] S.H. Ng, S.Y. Chew, J. Wang, D. Wexler, Y. Tournayre, K. Konstantinov, H.K. Liu, J. Power Sources 174 (2007) 1032.
[21] B. Alonso, J. Livage, J. Solid State Chem. 148 (1999) 16.
[22] I. Taniguchi, D. Song, M. Wakihara, J. Power Sources 109 (2002) 333.
[23] Y.N. Ko, H.Y. Koo, J.H. Kim, J.H. Yi, Y.C. Kang, J.H. Lee, J. Power Sources 196 (2011) 6682.
[24] S.H. Park, Y.K. Sun, Electrochim. Acta 50 (2004) 431.
[25] Y.N. Ko, J.H. Kim, Y.J. Hong, Y.C. Kang, Mater. Chem. Phys. 131 (2011) 292.

[26] C.Q. Feng, S.Y. Wang, R. Zeng, Z.P. Guo, K. Konstantinov, H.K. Liu, J. Power Sources 184 (2008) 485.
[27] Y. Chen, H. Liu, W.L. Ye, Scripta. Mater. 59 (2008) 372.
[28] C.K. Chan, H. Peng, R.D. Twesten, K. Jarausch, X.F. Zhang, Y. Cui, Nano Lett. 7 (2007) 490.
[29] J. Muster, G.T. Kim, V. Krstic, J.G. Park, Y.W. Park, S. Roth, M. Burghard, Adv. Mater. 12 (2000) 420.
[30] J. Liu, H. Xia, D. Xue, L. Lu, J. Am. Chem. Soc. 131 (2009) 12086.
[31] T. Watanabe, Y. Ikeda, T. Ono, M. Hibino, M. Hosoda, K. Sakai, T. Kudo, Solid State Ionics 151 (2002) 313.